Proceedings of the 3rd IASME/WSEAS Int. Conf. on HEAT TRANSFER, THERMAL ENGINEERING AND ENVIRONMENT, Corfu, Greece, August 20-22, 2005 (pp110-114)

# Numerical Study of Particle Deposition in a Channel Flow with a Built-In Cylinder

* M. SALMANZADEH[1], A. SOLTANI GOHARRIZI[2] and M. RAHNAMA[3]
*Author for correspondence
[1]Department of Mechanical Engineering
Islamic Azad University of Kerman
P.O. Box: 76135-858-Kerman
[2]Department of Chemical Engineering
Shahid Bahonar University of Kerman
[3]Department of Mechanical Engineering
Shahid Bahonar University of Kerman
IRAN

*Abstract:* - Particle trajectory and deposition in a channel flow with a rectangular cylinder was studied numerically. The continuity and Navier-Stokes equations were discretized using finite volume method. The particle equation of motion including the stokes drag force was used for determining lagrangian particle trajectory. Effects of aspect ratio, blockage ratio and stokes number on particle deposition on the cylinder front side has been studied for Re=200 and compared with previous work. The results showed that changing aspect ratio has no effect on particle deposition but the increase of blockage ratio and stokes number increases the deposition efficiency on front side of the cylinder.

*Key-Words:* - Particle trajectory-Rectangular cylinder-Channel flow

## 1 Introduction

The motion and deposition of particles in laminar and turbulent flows over various objects is important in numerous practical situations, consequently it has been studied by many investigators, both numerically and experimentally. In the early studies, analytical and experimental techniques employed for prediction of particle deposition over some obstructions. For example May and Clifford [1] examined the impaction of aerosol particles on cylinders, spheres, ribbons and discs experimentally. Golovin and Putnam [2] have calculated the target efficiency of a ribbon based on potential flow. Fuches [3], Davies [4], Friedlander and Johnstone [5], and Cleaver and Yates [6] provided semiempirical expression for particle mass flux from a turbulent stream to smooth surfaces. Besides the experimental studies, a large numbers of numerical studies on particle motion and deposition have been done specially in the recent years. Li et al. [7] studied aerosol particle deposition in an obstructed turbulent duct flow numerically. The effect of obstructions on the particle collection efficiency in a two stage electrostatic precipitator has been studied by Suh and kim [8]. Soltani et al. [9] have performed a numerical study of turbulent flow field, particle trajectory and deposition around a surface mounted ribbon. Brandon et al. [10] studied numerically the particle deposition on a square cylinder placed in a channel flow and investigated the effects of Stokes and Reynolds numbers on particle trajectory and deposition.. Yu et al. [11] investigated particle-laden turbulent flow over a backward-facing step by using large eddy simulation for the fluid phase and particle track model for particle motion. They considered the effects of both drag and gravitational forces on particle motion.

Although previous investigations have examined particle deposition in different flow configurations, we are not aware of any publication dealing with the effect of aspect ratio and blockage ratio on particle deposition in a channel flow with a built-in rectangular cylinder. In the present work particle trajectory and deposition in a channel flow with rectangular cylinder was studied numerically. Effect of aspect ratio, blockage ratio and stokes number on particle trajectories and cylinder front side particle deposition efficiency has been studied for Re=200 and compared with previous work. .

## 2 Problem Formulation

### 2.1 Nomenclature

$u_i$ instantaneous fluid velocity

$u_i$ mean flow fluid velocity

$p$ pressure

$u_m$ maximum velocity at inlet(m/s)
$u_i^p$ particle velocity
$x_i$ particle position
$t$ time
$d$ particle diameter
$g$ acceleration of gravity
$s$ particle to fluid density ratio
$B$ rectangular cylinder height
$W$ rectangular cylinder length
$H$ channel height
$L$ channel length
$Ar$ aspect ratio *W/B*
$Br$ blockage ratio *B/H*
$\lambda$ fluid molecules mean free path
$\nu$ kinematic viscosity ($m^2/s$)

### 2.2 Physical domain and equation of fluid flow

Fig. 1 shows the physical domain selected for study. A rectangular cylinder with height (B) and length (W) is centrally located in a channel with height (H) and length (L). L is 24B.

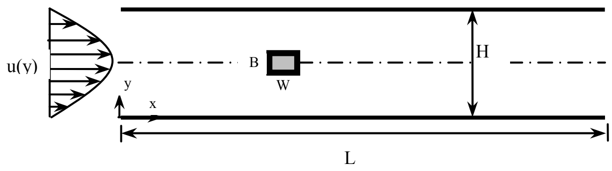


Fig.1: Physical domain

The equations governing the unsteady incompressible fluid flow are the continuity and Navier-Stokes equations, which can be written in the nondimensional form as:

$$u_{i,i} = 0 \tag{1}$$

$$\frac{\partial u_i}{\partial t} + u_j u_{i,j} = -p_{,i} + \frac{1}{\mathrm{Re}} u_{i,jj} \tag{2}$$

Here Re defined as $\mathrm{Re} = \frac{B.u_m}{\nu}$ . The equations are normalized by using B as the length scale, $u_m$ as the velocity scale and $\frac{B}{u_m}$ as the time scale.

The governing equations were discretized using a finite volume method with the staggered grid. The convective terms were discritized using central difference scheme.

The convective and diffusive fluxes in the momentum equation were treated explicitly in the present computations. A third order Runge-Kutta algorithm is used for the time integration in conjunction with the classical correction method at each sub-step. The continuity equation (1) and the pressure gradient term in the momentum equation (2) are treated implicitly. This method called semi-implicit fractional step, provides an approach that does not use pressure in the predictor step as in the pressure corrector method (such as the well-known SIMPLE family of algorithms). The linear system of pressure is solved by an efficient conjugate gradient method with preconditioning. Further details on the numerical method are given in Suksangpanomrung [12].

At the channel entrance the x-component velocity has a parabolic profile with maximum velocity $u_m$ and the y-component velocity is zero. At the channel exit, a continuous outflow condition is prescribed. On the top and bottom walls of the channel as well as the cylinder boundaries, no-slip boundary conditions are prescribed.

### 2.3 Particle equation of motion

The nondimentionalized equation of motion of small aerosol particle is given by:

$$\frac{du_i^p}{dt} = \frac{1}{stk}(\overline{u}_i - u_i^p) - \frac{1}{Fr^2}(1 - \frac{1}{s}) \tag{3}$$

$$\frac{dx_i}{dt} = u_i^p \tag{4}$$

Where

$$stk = \frac{s.d^2.c_c.u_m}{18.\nu.B} \quad , \quad Fr = \frac{u_m}{\sqrt{B.g}} \tag{5}$$

$C_c$ is the Stokes-Conningham slip correction given as:

$$c_c = 1 + \frac{2\lambda}{d}(1.257 + 0.4 e^{-1.1\frac{d}{2\lambda}}) \tag{6}$$

The first term on the right hand side of Eq. (3) is the drag force due to relative motion between particles and fluid. The second term is gravitational force. The drag force is always present and generally a dominant force.

Fourth order Runge-Kutta algorithm has been used for solving Eqs. (3) and (4).

## 3 Results

To check the accuracy of the flow field, computations were also performed for a rectangular cylinder placed in the middle of a channel with

Proceedings of the 3rd IASME/WSEAS Int. Conf. on HEAT TRANSFER, THERMAL ENGINEERING AND ENVIRONMENT, Corfu, Greece, August 20-22, 2005 (pp110-114)

blockage ratio of 1/8 at Reynolds numbers of 50, 100, 150 and 200. Fully developed parabolic velocity profile was assumed at the inlet. As the flow field is unsteady with vortex shedding for Re>50, a plot of vorticity field was shown in Fig. 2 to represent the relatively complex flow appeared in this geometry.

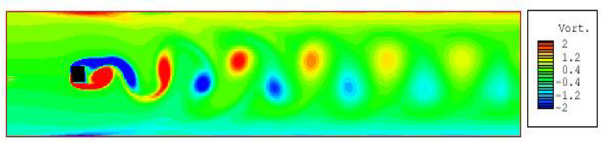


Fig.2: Instantaneous vorticity field for a square cylinder at Re=200

The value of Strouhal number was compared with that obtained by Breuer et al. [13] in Fig. 3. As it is observed in this figure, the differences between present computations and those of ref. [13] were small.

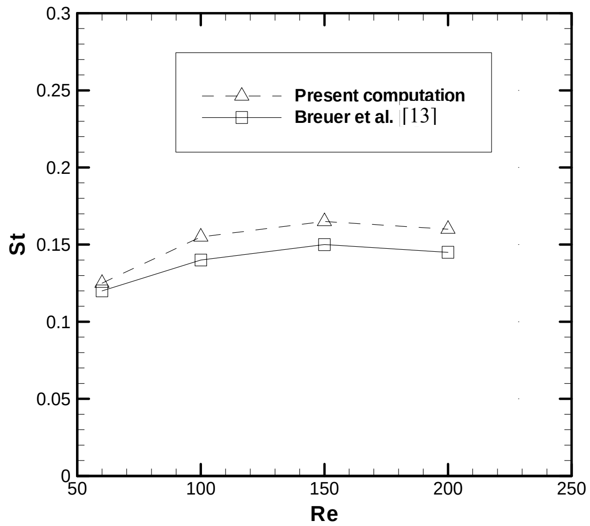


Fig. 3: Variation of Strouhal number with Reynolds number for square cylinder

Fig. 4 shows the mean streamlines for Re=200 and Ar=2 and Br=0.25. As it is seen two recirculation regions are formed back of the cylinder.

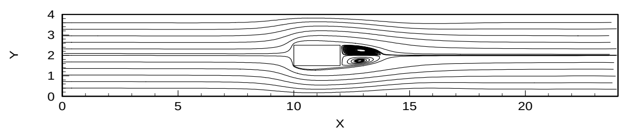


Fig.4: Mean flow velocity vectors and streamlines plots for Re=200 , Ar=2, Br=0.25

Particles with prescribed stokes numbers were injected with uniform distribution from the inlet of the channel and their trajectories were calculated in the absence of gravity.

Fig. 5 shows the trajectories of some particles at different stokes numbers and Br=0.25, Ar=2. Due to particles inertia, they do not follow the streamlines of the fluid and depending on their deviation from the streamlines, they might be caught by the cylinder and deposited on it. The deviation of particles form fluid streamlines depends on their stokes number. As can be seen from Fig. 5, for large stokes numbers the deviation is large and for small stokes numbers it is small and particles follow the streamlines to some extent.

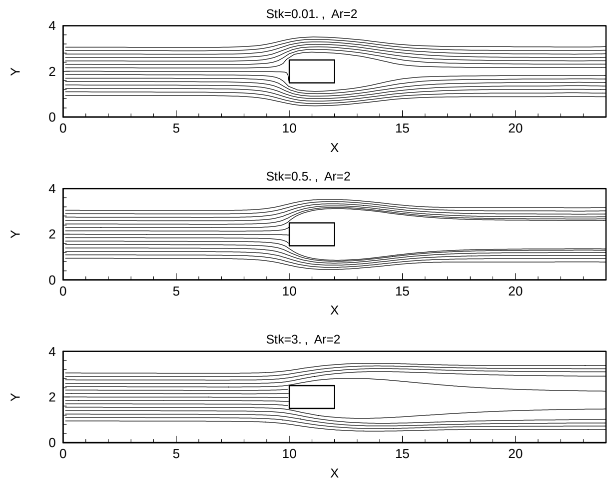


Fig. 5: Particle trajectories for Re=200, Br=0.25, Fr=∞

Particle deposition efficiency on front side of the cylinder is defined as:

$$\eta = \frac{\textit{number of particles deposited on the front side}}{\textit{number of particles entering the projected area}}$$

201 particles of given stokes number injected uniformly from 5B upstream of the cylinder at the projected area and the deposition efficiency has been calculated. This was done for different stokes numbers.

Fig. 6 shows the variation of deposition efficiency as a function of stokes number for three different aspect ratios along with the data obtained by Brandon et al. [10]. As it is observed in this figure the present computations follow the same trend as those of ref. [10]. It should be noted that the deposition efficiencies computed for stk<0.5 have lower values than those obtained by Brandon et al. [10]. The reason for such behaviour is that, at small stokes numbers the dominant deposition mechanism is diffusion by Brownian motion that in our study and previous work it has not been investigated. In the absence of Brownian motion the impaction is the dominant mechanism for deposition, therefore, the number of deposited particles approaches zero when the stokes number is small, so it seems that the present work is more accurate than the previous work [9] specially at small stokes numbers. It can also be seen in the experimental work of May and Clifford [1], deposition efficiency of particle on a ribbon at small stokes number approaches zero.

Fig.7 shows the variation of deposition efficiency versus stokes number for three different blockage ratios. As it shows change of blockage ratio from 0.1 to 0.5, increases the particle deposition efficiency for all stokes numbers.

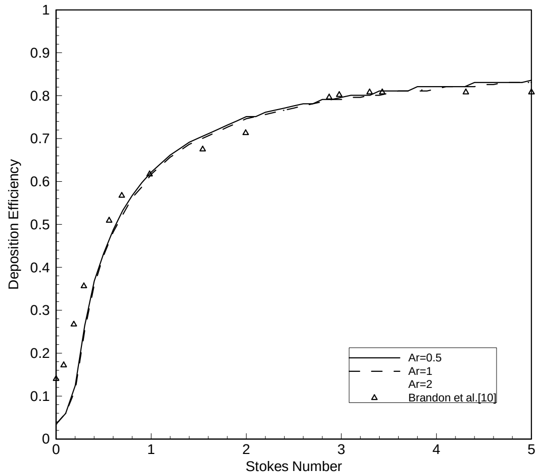


Fig. 6: Variation of particle deposition with Stokes number for 3 different aspect ratios.

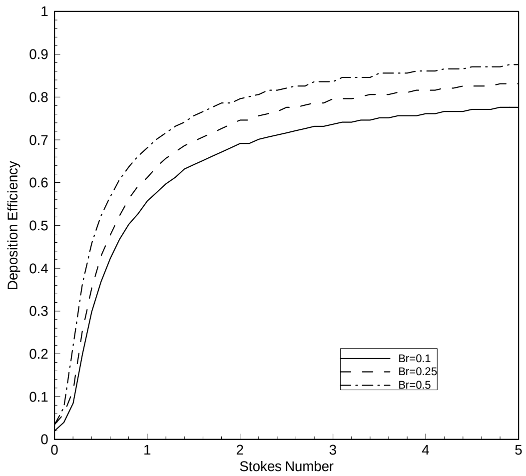


Fig. 7: Variation of particle deposition with Stokes number for 3 different Blockage ratios.

The amount of deposition increases sharply as the stokes number is increased from low values to unity. For 1<stk<3, the particle deposition increases relatively slowly with stokes number. For stk=3, the deposition becomes essentially independent of the stokes number. The rising trend of deposition efficiency with increasing stokes number, is the same for all three blockage ratios.

## 4 Conclusion

Particle trajectory and deposition in a channel flow with a rectangular cylinder was studied numerically for Re=200 with the effect of blockage ratio, stokes number and aspect ratio.

The increase of stokes number increases the deposition efficiency especially for 0 <stk<1 and for larger stokes numbers, this rising trend is slow.

Aspect ratio has no serious effect on the cylinder front side deposition but the increase of blockage ratio increases deposition efficiency.

*References:*

[1] May, K. R., and Clifford, R, The Impaction of Aerosol Particles on cylinder, sphere, Ribbons and disks, *Ann. Occup. Hyg,* Vol.10, 1967, p.83.

[2] Golovin, M. N., and Putnam, A. A., Inertial Impaction On Single Elements, *Ind.Engng. Chem. Fundam*, Vol.1, 1962, p.264.

[3] Fuches, N. A., *The Mechanics of Aerosol*, Pergamon Press, 1964

[4] Davies, C. N., *Aerosol Science*, Academic Press, London, 1966

[5] Friedlander, S. K., and Johnstone, H. H., Deposition Of Suspended Particles from Turbulent Gas Stream, *Ind. Eng. Chem*, Vol.49, 1957, p.1151.

[6] Cleaver, J. W., and Yates, B., A Sublayer Model for the Deposition of Particles from a Turbulent Flow, *Chem. Eng. Sci,* Vol. 30, 1975, p.983.

[7] Li, A., Ahmadi, G., Bayer, R. G., and Gaynes, M. A., Aerosol particle deposition in an Obstructed Turbulent Duct flow, *J. Aerosol Sci.*, Vol.25, 1994, p.91.

[8] Suh, Y. J., and Kim, S. S., Effect of Obstructions on the Particle Collection Efficiency in a Two-Stage Electrostatic Precipitator, *J. Aerosol Sci.*, Vol.27, 1996, p.61.

[9] Soltani Goharrizi, A., Taheri, M., and Fathikalajahi, J., Prediction of Particle Deposition from a Turbulent Stream around a Surface-Mounted Ribbon, *J. Aerosol Sci.*, Vol.29, 1998, p.141.

[10] Brandon, D. J. and Aggarwal, S.K., A Numerical investigation of particle deposition on

a square cylinder Placed In a Channel Flow, *J. Aerosol Sci.*, Vol.34, 2001, p.340.

[11] Yu, K.F., K. S. Lau, K.S. and Chan, C.K., Numerical Simulation of Gas-Particle flow in a Single-Side backward-Facing Step Flow, *J. of Computational and Applied Mathematics*, Vol.163, 2004, p.319.

[12] Suksangpanomrung, A., Investigation of unsteady separated flow and heat Transfer using direct and large-eddy simulations,*PhD Thesis*, Department of Mech. Eng., University of Victoria, Canada, 1999.

[13] Breuer, L., Bernsdorf, M., Zeiser, J. and Durst, F., Accurate Computations of the Laminar Flow Past a Square Cylinder Based on Two Different Methods: Lattice- Boltzmann and Finite-Volume, *Int. J. Heat and Fluid Flow*, Vol. 21, 2000, p.186.